References

1. J.-I. Jin, J.-S. Kang, B.-W. Jo and R. W. Lenz, *Bull. Korean Chem. Soc.*, **4**, 176 (1983).
2. J.-I. Jin, Y.-S. Chung, R. W. Lenz and C. Ober, *Bull. Korean Chem. Soc.*, **4**, 143 (1983).
3. J.-I. Jin, E.-J. Choi, S.-C. Ryu and R. W. Lenz, *Polym. J. (Japan)*, **18**, 63 (1986).
4. J.-I. Jin, C.-M. Sung and B.-W. Jo, *Bull. Korean Chem. Soc.*, **6**, 40 (1985).
5. J.-I. Jin and J.-H. Park, *Mol. Cryst. Liq. Cryst.*, **110**, 293 (1984).
6. B.-W. Jo, T.-K. Lim and J.-I. Jin, *Mol. Cryst. Liq. Cryst.*, **157**, 57 (1988).
7. A. C. Griffin and T. R. Britt, *J. Amer. Chem. Soc.*, **103**, 4957 (1981).
8. J. A. Buglione, A. Roviello and A. Sirigu, *Mol. Cryst. Liq. Cryst.*, **106**, 169 (1984).
9. H. Sackmann and D. Demus, *Mol. Cryst. Liq. Cryst.*, **21**, 239 (1973).
10. J.-I. Jin, H.-T. Oh and J.-H. Park, *J. Chem. Soc., Perkin Trans. II.*, 343 (1986).
11. J. B. Flannery, Jr., and W. Haas, *J. Phys. Chem.*, **74**, 3612 (1970).
12. G. W. Smith, Z. G. Gardlund and R. J. Curtis, *Mol. Cryst. Liq. Cryst.*, **19**, 327 (1973).
13. G. W. Gray and P. A. Winsor, Ed., 'Liquid Crystals & Plastic Crystals', Vol. 1, Ellis Horwood Ltd., London, 1974, pp.123-124.
14. J. C. W. Chien, R. Zhou and C. P. Lillya, *Macromolecules*, **20**, 2340 (1987).

CO_2 Laser Induced Decomposition of 1-Bromo-3-Chloropropane

Byoung Soo Chun, Nam Woong Song, and Kwang Yul Choo*

Department of Chemistry, Seoul National University, Seoul 151-742. *Received December 21, 1989*

We have studied the Infrared Multiphoton Dissociation (IRMPD) of 1-bromo-3-chloropropane by using the pulsed CO_2 laser. The product yields and the HCl/HBr branching ratios in IRMPD of $BrCH_2CH_2CH_2Cl$ are studied under the focused beam geometry as a function of buffer gas (He) pressure, laser energy, and photolysing wavelength. It is observed that the total dissociation yield has a laser energy dependence of 1.8-2.0 power order and the branching ratio is very slightly dependent on the pulse energy for the laser lines employed. The dependences of total dissociation yield and branching ratio on the buffer gas pressures show that the dissociation yield monotonically decreases and the branching ratio slightly decreases with the increase of the buffer gas pressure. The Energy-Grained Master Equation (EGME) was applied to explain the laser pulse energy and the buffer gas pressure(He) dependence of the dissociation yield and the branching ratio.

Introduction

The infrared multiphoton dissociation(IRMPD) of polyatomic molecules with two or more dissociation channels has been an important subject for understanding of multiphoton absorption and decomposition process in the gas phase[1,2].

Molecular elimination reactions of halogenated compounds with competing reaction channels in the IRMPD has been reported by several workers[1,3-9]. Halogenated compounds generally undergo unimolecular processes such as rearrangement, elimination and homolytic bond fission. Homolytic bond fission, relatively higher energy channel than molecular elimination, is preferred at a very high excitation energy level. It can be induced by highly intense IR laser[10]. Many workers have shown that the molecular elimination channel is generally more predominant in IRMPD of halogenated compounds[1,4].

The branching ratio of products can be varied by experimental conditions (fluence, pressure of buffer gases, beam geometry, laser frequency, and the number of pulses). Colussi *et al.*[11] reported that the HCl/DCl ratio in IRMPD of CH_2DCH_2Cl was independent of experimental conditions. However, it was generally observed that the branching ratio was affected by experimental parameters. Yano *et al.*[3] reported that, in IRMPD of CF_2ClCH_2Cl, the branching ratio of products (HF/HCl) decreased with the increase of the pulse energy, and increased with increasing the buffer gas pressure (Ar). Benson *et al.*[4] also reported that the branching ratio (HCl/DCl) in the photolysis of CH_2DCH_2Cl decreased with increasing pressure in range of 0-5 torr and reached a plateau for pressures higher than 5 torr.

$BrCH_2CH_2CH_2Cl$ may be considered to be decomposed *via* HBr and HCl molecular elimination followed by a secondary photolysis into allene.

$$BrCH_2CH_2CH_2Cl \xrightarrow{nh\nu} CH_2CHCH_2 + HBr$$

$$BrCH_2CH_2CH_2Cl \xrightarrow{nh\nu} CH_2CHCH_2Br + HCl$$

$$CH_2CHCH_2Cl \xrightarrow{nh\nu} CH_2CCH_2 + HCl$$

$$CH_2CHCH_2Br \xrightarrow{nh\nu} CH_2CCH_2 + HBr$$

The secondary photolysis has been recognized as a significant process in IRMPD, especially for the large molecules. It is, thus, necessary to study IRMPD of allyl chloride and allyl bromide, the primary dissociation products of $BrCH_2CH_2CH_2Cl$ photolysis, in order to fully understand the IRMPD of $BrCH_2CH_2CH_2Cl$.

The irradiation zone becomes optically inhomogeneous

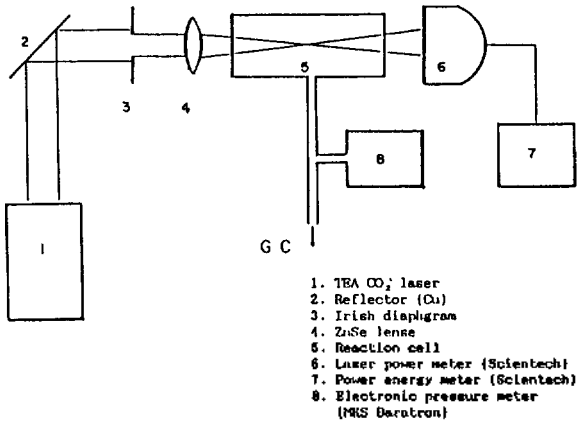

Figure 1. Schematic diagram of the experimental set up. 1. TEA CO_2 laser; 2. Reflector (Cu); 3. Irish diaphgram; 4. ZnSe lense; 5. Reaction cell; 6. Laser power mater (Scientech); 7. Power energy meter (Scientech); 8. Electronic pressure meter (MKS Baratron).

with focusing geometry. Under this condition, it is known that the dissociation yield has a laser energy dependence of 3/2 order. It was interpreted in terms of a simple threshold model[13,14].

The theoretical models for IRMPD have been reported by many workers[15-18]. Particularly, the application of Energy-Grained Master Equation (EGME) to the IR multiphoton process has been theoretically justified[18] and applied to the numerous systems. Quack's case B.[18] applied to transitions between two levels in which the intramolecular relaxation rates are fast between states in a particular level. The ratio of up- and down-transition rates is determined by detailed balance using the state densities of the two energy levels, as in the incoherent excitation model. EGME has adequately reproduced such experimental data as the dependence of product yield on the pressure and laser fluence, and has, in addition, provided information on the distribution of population in the vibrational manifold as a function of time. EGME was applied to explain the laser energy and the pressure dependence in our work.

Experimental

A schematic diagram of the experimental set up is shown in Figure 1. A TEA CO_2 laser, Tachisto 215G, was used as a radiation source. The laser output consisted of a 40 nsec (FWHM) gain switched spike followed by low intensity tail of 500 nsec. Pulse energies were determined with Scientech calorimeter (Scientech 36-2001) located just behind the exist window and its loss was corrected by window transmittance (0.92 and 0.93 at 10P(20) and 10P(12), respectively).

In absorption measurements, the unfocused laser beam was passed through an absorption cell (49 cm long, 2.6 cm inside diameter) that was made of clean pyrex tube fitted with NaCl Brewster angle windows. The transmittance of $BrCH_2CH_2CH_2Cl$ in the cell was obtained by measuring transmitted energies with and without $BrCH_2CH_2CH_2Cl$ in the optical path. Irish diaphgram was used to reduce the beam size and to provide a more homogeneous beam.

Reactions were carried out in a cell consisting of cylindrical Pyrex tube of 10 cm length and 2 cm diameter with both ends fitted with NaCl windows. A ZnSe lense (focal length = 15 cm) was used to focus the beam into the the center of reaction cell. Pulse energies were varied with polyethylene sheets, and the pulse repetition rate was set at 1 Hz for all run. The reaction products were analyzed by Gas Chromatography (Yanaco G-80) using flame ionization detector (FID). The separation of products was achieved with Hall M-18-OL column of 2.4 m length at 110 °C. Product identification was based on the comparison of retention times of unknown peaks with those of authentic samples. All pressures were monitored by the MKS Baratron transducer. Irradiation lines used were 10P(20) 944.2 cm^{-1} and 10P(12) 951.2 cm^{-1}.

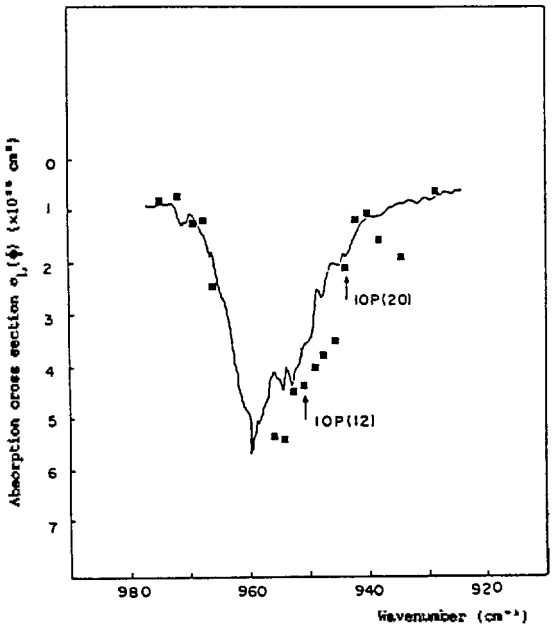

Figure 2. Wavelength dependence of $\sigma_L(\phi)$ of $BrCH_2CH_2CH_2Cl$ at constant fluence of 2.3×10^{-2} J/cm^2(●). IR absorption spectrum (solid line) is shown for comparision. (Transmittance in arbitrary unit).

The reactant, $BrCH_2CH_2CH_2Cl$, and the principal product olefins, CH_2CHCH_2Cl and CH_2CHCH_2Br, were obtained from Aldrich Chemical Co. All reactants were degassed and transferred to reaction cell after several freeze-pump-thaw cycles.

Results and Discussion

1. The Measurements of an Absorption Cross Section.

IR spectrum of $BrCH_2CH_2CH_2Cl$ showed the absorption band at near 950 cm^{-1}. The absorption cross sections at several CO_2 laser lines were calculated by using the Beer-Lambert's law.

$$\sigma_L(\phi) = -\frac{1}{Nl}\ln(\phi/\phi_0)$$

ϕ : Energy passed through the cell with the sample
ϕ_0 : Energy passed through the cell without the sample
N : Concentration (molecules/cm^3)
l : Cell length (cm)

As shown in Figure 2, the shape of absorption cross sections measured with CO_2 laser lines is in agreement with that

Table 1. The Dependence of Relative Product Yields on the Pulse Energy in IRMPD of $BrCH_2CH_2CH_2Cl$

For 10P(20) line

Energy(J) ($\times 10^1$)	Dissociation yield($\times 10^4$) per pulse	Allene	Allyl chloride	Allyl bromide	Total dissociation yield(%)
5.23	4.22	123	100	35.3	34.4
4.57	3.28	115	100	34.8	28.0
4.08	2.72	101	100	34.7	23.8
3.60	2.35	96.7	100	33.0	20.9
2.94	1.65	84.3	100	32.9	15.2
1.96	0.812	60.0	100	35.0	7.8
1.53	0.387	34.8	100	30.4	3.8

*The reactant pressure: 0.56 torr. The number of pulses: 1000.

For 10P(12) line

Energy(J) ($\times 10^1$)	Dissociation yield($\times 10^4$) per pulse	Allene	Allyl chloride	Allyl bromide	Total dissociation yield(%)
4.52	4.18	115	100	34.3	34.2
3.93	3.44	105	100	33.6	29.1
3.38	2.63	93.1	100	33.3	23.1
2.75	1.63	85.5	100	31.9	15.0
2.20	1.30	70.0	100	33.3	12.2
1.66	0.672	51.4	100	34.3	6.5
1.27	0.274	29.4	100	29.4	2.7

*The reactant pressure: 0.56 torr. The number of pulses: 1000.

Table 2. The Dependence of Relative Product Yields on the Number of Pulses in IRMPD of $BrCH_2CH_2CH_2Cl$

For 10P(20) line

Number of pulses	Total dissociation yield(%)	Allene	Allyl chloride	Allyl bromide
200	7.5	75.0	100	33.3
400	12.6	79.7	100	33.9
600	17.9	92.4	100	34.2
800	21.0	105	100	34.1
1000	28.1	115	100	35.7

*The pulse energy: 4.57×10^{-1} J/pulse. The reactant pressure: 0.56 torr.

For 10P(12) line

Number of pulses	Total dissociation yield(%)	Allene	Allyl chloride	Allyl bromide
200	7.6	75.7	100	27.9
400	12.7	81.7	100	30.0
600	17.7	93.7	100	30.4
800	23.1	96.0	100	32.7
1000	30.3	104	100	34.6

*The pulse energy: 3.93×10^{-1} J/pulse. The reactant pressure: 0.56 torr.

Table 3. The Dependence of Relative Product Yields on the Buffer Gas (He) Pressure in IRMPD of $BrCH_2CH_2CH_2Cl$

For 10P(20) line

Pressure of He (torr)	Dissociation yield($\times 10^4$) per pulse	[a]Allene	Allyl chloride	[b]Allyl bromide	Total dissociation yield(%)
0	3.48	111	100	36.1	29.4
0.58	2.87	113	100	34.7	25.0
1.33	2.51	121	100	34.5	22.2
2.53	2.14	132	100	32.9	19.3
3.90	1.85	142	100	30.6	16.9
6.30	1.28	151	100	27.9	12.0
9.70	1.23	172	100	25.6	11.6
13.0	0.747	187	100	26.1	7.2

*The pulse energy: 4.57×10^{-1} J/pulse. The reactant pressure: 0.56 torr. The number of pulses: 1000.

For 10P(12) line

Pressure of He (torr)	Dissociation yield($\times 10^4$) per pulse	Allene[a]	Allyl chloride	Allyl[b] bromide	Total dissociation yield(%)
0	3.28	104	100	33.6	27.9
0.58	2.75	108	100	34.3	24.0
1.42	2.26	117	100	33.3	23.3
2.49	1.79	120	100	32.3	16.4
3.90	1.64	138	100	32.1	15.1
6.31	1.10	154	100	27.0	10.4
9.50	1.10	147	100	26.3	10.4

*The pulse energy: 3.93×10^{-1} J/pulse. The reactant pressure: 0.56 torr. The number of pulses: 1000. [a,b]represent the relative yields when the amount of allyl chloride was taken to be 100.

of IR spectrum at fluence of 2.3×10^{-2} J/cm^2. In dissociation experiments, the irradiation frequencies of 10P(12) and 10P (20) laser lines were selected.

2. Dissociation Experiment.

$BrCH_2CH_2CH_2Cl$, CH_2CHCH_2Cl and CH_2CHCH_2Br were photolyzed at two different wavelengths (10P(20) and 10P (12)); 10.591 and 10.513 μm. 10P(20) and 10P(12) correspond to the red and the near maximum of absorption band of 10 μm, respectively. When gaseous $BrCH_2CH_2CH_2Cl$ is irradiated with the 10P(20) and 10P(12), the dominant products (>95% of total dissociation yield) found were allyl chloride, allyl bromide and allene. In addition, several very minor unidentified peaks were also observed. The numbers shown in Table 1,2 and 3 are the relative yields of products when the allyl chloride yield is taken as 100.

1) Energy Dependence. The total dissociation yields per pulse in the photolysis of $BrCH_2CH_2CH_2Cl$ were examined as a function of the number of pulses, excitation laser wavelengths, and laser energies. The total dissociation yield per pulse is given by the expression.

$$\frac{d[A]}{dn} = -\alpha[A] \quad (1)$$

Assuming that α is independent of the extent of reaction, then Eq. (1) can be integrated to give

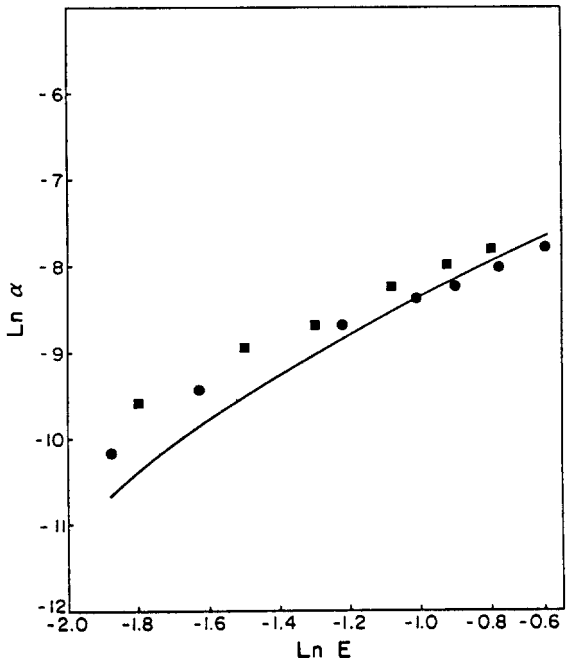

Figure 3. The dependence of the total dissociation yield(α) on the pulse energy(E) in IRMPD of $BrCH_2CH_2CH_2Cl$. ●: Irradiation with 10P(20) line. Slope(m) = 1.86 ± 0.24. ■: Irradiation with 10P(12) line. Slope(m) = 2.06 ± 0.35. The solid line represents the calculated result for 10P(20) line.

$$\alpha = -(1/n)\ln([A]/[A_0]) = -(1/n)\ln\left(\frac{[A]_0 - \Sigma P_i}{[A]_0}\right)$$

Where n is the number of pulses, $[A]_0$ and $[A]$ are the concentrations before and after photolysis and P_i denotes the concentration of the ith product. α is the decomposition yield per pulse or the ratio of the effective decomposition volume to the cell volume. The dependence of the total dissociation yield (α) on the pulse energy is shown in Figure 3. The log-log plots are linear and obey the relationship $\alpha \propto E^{\beta}$. From the slopes, the values of the exponent are found to be β = 1.86 ± 0.24 at 10P(20) and β = 2.06 ± 0.35 at 10P(12). These values have little difference within experimental error. However, the exponent β is slightly larger than the 3/2 power energy dependence[4,14,19]. The deviation from the 3/2 power energy dependence also have been observed elsewhere[3,20]. Several workers interpreted the energy dependence on IRMPD by geometrical effects in a reaction cell[3,6,14,20]. The 3/2 power energy dependence[14] is based on the assumption that all molecules in a conical zone where fluence is above some critical value dissociate with a unit probability and ignore any reactions outside this zone.

Allene, one of the major products in our experiments, may be produced *via* the following reaction steps.

I) secondary photolysis of allyl bromide and allyl chloride.

II) successive elimination of HCl and HBr from $BrCH_2CH_2CHCl$ within one pulse.

If allyl bromide and allyl chloride don't undergo secondary photolysis, the relative yield of allene must be independent of the number of pulses. As shown in Figure 4, the relative yield of allene increases as the number of pulses increases. This suggests that allyl chloride and allyl bromide, the primary dissociation products of $BrCH_2CH_2CH_2Cl$, undergo the secondary photolysis producing allene.

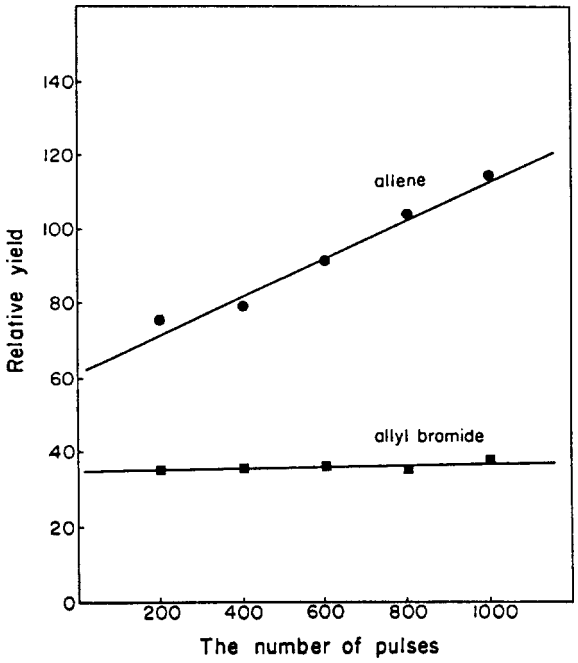

Figure 4. The dependence of relative product yields on the number of pulses in IRMPD of $BrCH_2CH_2CH_2Cl$.

As also shown in Figure 4, the relative yield of allene extrapolated to zero number of pulses does not become zero, indicating some allene also seems to be produced by a successive elimination of HCl and HBr within a pulse. Since allene is a product of a successive elimination of HCl and HBr, highly excited parent molecules are responsible for the formation of allyl chloride or allyl bromide with sufficient internal energies. Then, the primary products (*i.e.*, excited allyl chloride or allyl bromide) can be decomposed to allene by absorbing only a few photons within the duration of the pulse. Since the formation of allene *via* a successive elimination requires a formation of highly excited $BrCH_2CH_2CH_2Cl$, the production of allene is expected to be less affected by the increase of buffer gas pressures than that of allyl bromide and allyl chloride. As shown in Table 3, the relative yield of allene formation in comparison with allyl chloride increases with increasing He pressure, indicating that allene is less deactivated than allyl chloride. From the above considerations, the sources of allene are not only originated from the secondary photolysis of allyl chloride and allyl bromide, but also from the successive elimination of HCl and HBr from $BrCH_2CH_2CH_2Cl$ within one pulse.

The branching ratio(R) is defined as follows;

$$R = \frac{[HCl]}{[HBr]} = \frac{[\text{Allyl bromide}]}{[\text{Allyl chloride}]}$$

The branching ratios were obtained by monitoring the concentrations of allyl chloride and allyl bromide. The experimentally observed branching ratios may have unwanted contribution from the possible secondary elimination of HCl and HBr from allyl chloride or allyl bromide. Since there was little detailed quantitative information on the allene production to correct the observed branching ratio, the observed branching ratio was not corrected.

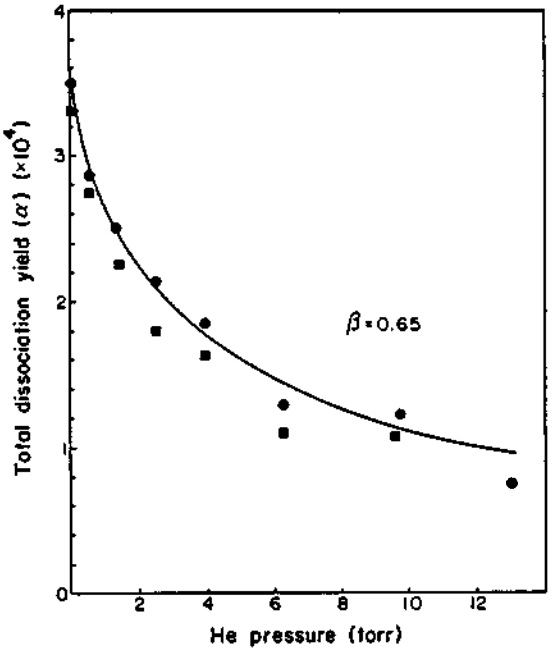

Figure 5. The dependence of total dissociation yields(α) on the buffer gas(He) pressures in IRMPD of $BrCH_2CH_2CH_2Cl$. ●: Irradiation with 10P(20) line. Laser energy: 4.57×10^{-1} J/pulse. ■: Irradiation with 10P(12) line. Laser energy: 3.93×10^{-1} J/pulse.

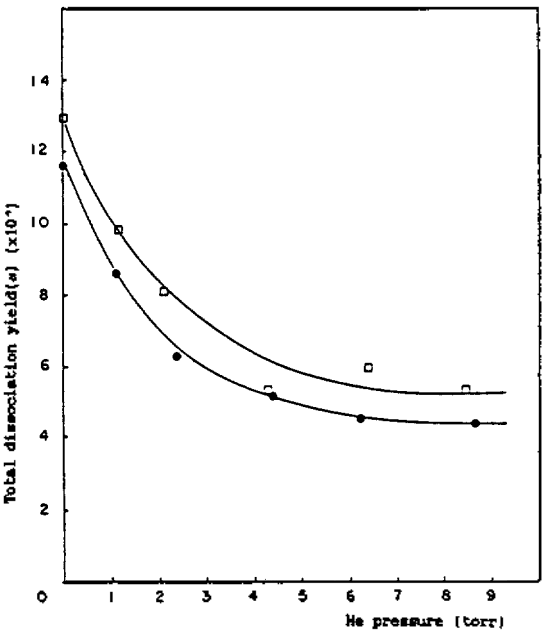

Figure 6. The dependence of the total dissociation yield(α) on the buffer gas(He) pressures in IRMPD of allyl bromide. ○: Irradiation with 10P(20) line. Laser energy: 4.52×10^{-1} J/pulse. ●: Irradiation with 10P(12) line. Laser energy: 3.93×10^{-1} J/pulse.

2) Secondary Photolysis. The IRMPD of allyl chloride and allyl bromide was examined as a function of the pulse energies and buffer gas pressures(He). From the dependence of the total dissociation yield on pulse energy for allyl chloride and allyl bromide dissociation, the exponent values(β) for allyl chloride were found to be $\beta = 1.65 \pm 0.18$ for 10P(20) and $\beta = 1.61 \pm 0.28$ for 10P(12). For allyl bromide, the exponent values(β) were $\beta = 1.78 \pm 0.25$ for 10P(20) and $\beta = 2.12 \pm 0.31$ for 10P(12). IRMPD of allyl chloride almost obey 3/2 power energy dependence, which can be interpreted by the simple threshold model.

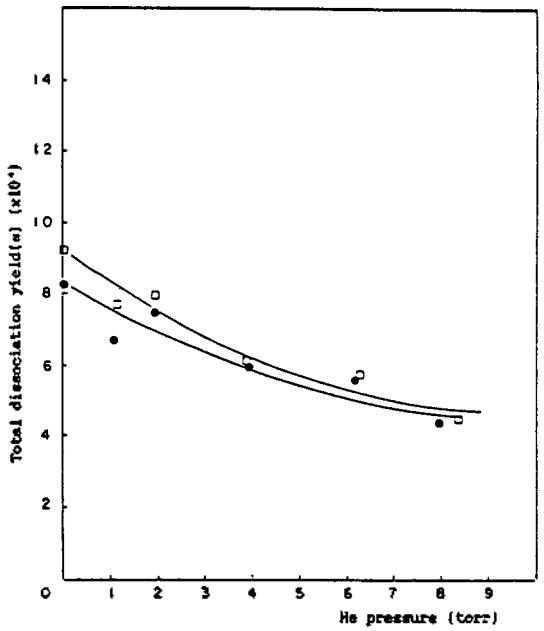

Figure 7. The dependence of the total dissociation yield(α) on the buffer gas(He) pressures in IRMPD of allyl chloride. ○: Irradiation with 10P(20) line. Laser energy: 4.53×10^{-1} J/pulse. ●: Irradiation with 10P(12) line. Laser energy: 3.93×10^{-1} J/pulse.

The dependence of total dissociation yields on the buffer gas pressure(He) are shown in Figures 6 and 7. As shown in Figures 6 and 7, the extent of the collisional deactivation for 10P(20) is similar to that of 10P(12) in IRMPD of allyl bromide and allyl chloride. But IRMPD of allyl bromide is more largely affected by buffer gas than that of allyl chloride.

3) Pressure Dependence & The Application of Energy-granied Master Equation (EGME). The total dissociation yield in IRMPD of $BrCH_2CH_2CH_2Cl$ was examined as a function of buffer gas pressure (He). Figure 5 shows that the total dissociation yields monotonically decreases with the increase of the buffer gas pressure. Any hole-burning effect that was observed frequently in IRMPD of small molecules[1,4,9] is not noticed here. This result shows that any collisional processes do not enhance the absorption of photons of reactants, but only deactivate the excited molecules.

If we assume that beam area at a point x centimeters from the focal point along the center line of the laser beam under the focusing geometry is given as follows

$$S(x) = \pi \left(\left(\frac{r_0 - r_f}{f} \right) x + r_f \right)^2$$

where r_0 is the incident beam radius on a lens of focal length f and r_f at focal point. Then, the experimentally observed decomposition yield per pulse(α) and the branching ratio(R) are given as following equations.

$$\alpha = V_r / V_c = 2 \int_0^1 P(\phi, x) S(x) \, dx / V_c \qquad (2)$$

where V_r and V_c are the effective decomposition volume

Table 4. Input Parameters in RRKM Calculation

Molecule	Activated complexes	
$BrCH_2CH_2CH_2Cl$	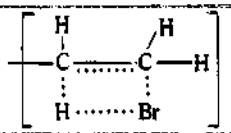	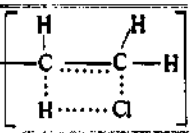
	E_a = 50.0 kcal/mol	E_a = 51.7 kcal/mol
frequencies in cm^{-1}(degeneracies)		
2950(6)	3000(5)	3000(5)
1450(5)	1350(5)	1350(5)
1220(3)	1170(3)	1170(3)
950(3)	950(3)	950(3)
760(3)	760(3)	760(3)
600(1)	600(1)	520(1)
500(1)	500(1)	430(1)
310(1)	360(1)	350(1)
170(1)	260(1)	300(1)
110(1)	150(1)	250(1)
82(1)	120(1)	170(1)
56(1)	82(1)	56(1)
$I_xI_yI_z$[a] 1.23×10^8	1.78×10^8	1.68×10^8
L[+b]	2	2

[a]in unit ($\times10^{-120}$ g^3cm^6). [b]reaction path degeneracy.

and cell volume, respectively and cell length is 21.

$$R=\int_0^1 R(\phi, x)\,P(\phi, x)\,S(x)\,dx/\int_0^1 P(\phi, x)\,S(x)\,dx \qquad (3)$$

where $R(\phi,x)$ and $P(\phi,x)$ are the branching ratio and reaction probability at a fluence ϕ, repectively.

The reaction probability ($P(\phi,x)$) at each fluence is assumed to be given as follows(14):

$$P(\phi, x)=1-\exp(-(\phi/\phi_r)^n) \qquad (4)$$

where ϕ_r is the fluence at which $P(\phi,x)$ is $1-1/e$. Either n or ϕ_r (or both) must also be functions of pressures. $P(\phi,x)$ is calculated by fitting the reaction probabilities obtained from the calculation of master equation at several fluences, in which ϕ_r and n are adjusted.

Master equation formulation

The differential equations used to model the multiphoton dissociation of $BrCH_2CH_2CH_2Cl$ are as follows:

$$\frac{dN_i}{dt}=R^a_{i-1}N_{i-1}+R^e_iN_{i+1}-(R^a_i+R^e_{i-1})N_i$$
$$+\beta\sum_i ZP_{ij}N_j-\beta\sum_j ZP_{ij}N_i-(k_i(HBr)+k_i(HCl))N_i$$

N_i : the population in the level i
R^a_i : the absorption rate constant from level i to $i+1$
R^e_i : the stimulated emission rate constant from level $i+1$ to i
β : collision efficiency
Z : the hard sphere collision frequancy
P_{ij} : the probability of a molecule making a transition from level j to level i upon collision
k_i : the dissociation rate constant from level i
k_i is set equal to zero when the energy is below the activation energy. The vibrational energy region was devided into equally spaced levels corresponding to laser frequency. The absorption rate constsants (R^a_i) were described by the following:

$$R^a_i=\sigma_iI(t)/h\nu$$

where σ_i is the absorption cross section for a transition from level i to $i+1$, $I(t)$ is the laser intensity, and $h\nu$ is photon energy. The stimulated emission rate constants were given by the detailed balance. The density of vibrational states was found by using the direct count method at low energy (<15 kcal/mol) and the Whitten-Rabinovitch approximation at high energy. Rate constants (k_i(HBr) and k_i(HCl)) were calculated according to the RRKM theory[21]. The input parameters in RRKM calculation are shown in Table 4. The branching ratio is largely affected by activation energies and Arrhenius A factors of the each reaction channels. The activation energy and A factor for HBr elimination are E_a = 50.0 kcal/mol and log A = 13.0, taken from the result in the pyrolysis of n-propyl bromide[22] and then, E_a and log A for HCl elimination is adjusted to reproduce the experimental results. The stepladder model[1,23] was used to determine the collisional transition probabilities P_{ij}. It is assumed that the average energy loss $\langle\Delta E_d\rangle$ is 2.7 kcal/mol corresponding to laser frequency in our calculation. We assumed that the laser has 40 ns rectangular pulse. Since the absorption cross section (σ_i) is unknown, it is assumed to fit the following function.

$$\sigma_i=\sigma_0(1+i)^{-m}$$

where m is adjustable parameter. We assumed the m value of 0.5 that was used in isopropyl bromide decomposition[24]. The EGME model was fit to the experimental data using an iterative fitting procedure in which σ_0 and the collision efficiency(β) were adjusted.

The above differential equations were solved by direct

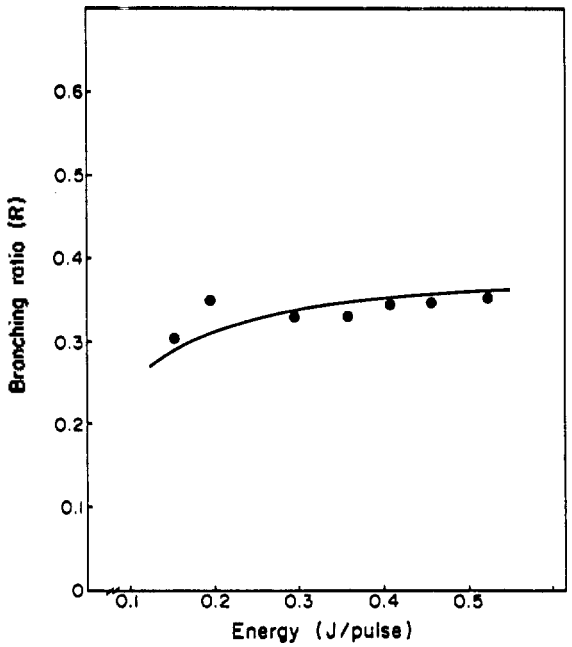

Figure 8. The dependence of branching ratio(R) on the pulse energy. The solid line represents the calculated result.

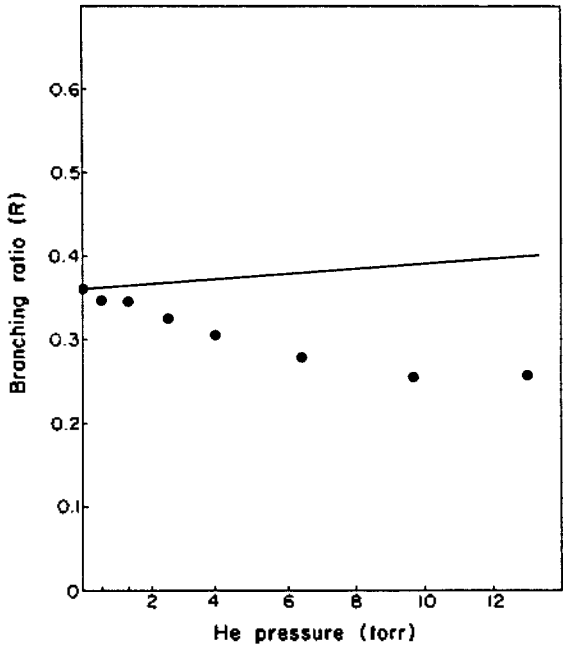

Figure 9. The dependence of branching ratio(R) on the buffer gas pressure(He). The solid line represents the calculated result.

numerical integration according to the Bulirsh-Stoer procedure[25]. The equations were integrated during the time with the laser "on", and the intergation was continued until the molecular population in levels above the lowest activation energy was negligible even when the laser was "off" (*i.e.*, K_i^a and K_i^e set equal to zero). The radius(r_f) at the focal point is 0.045 cm from the measurement of the beam divergence. The reaction probability which is calculated by EGME is fitted by using the equation 4. The best fitting is obtained by assuming that n is 3.13 and ϕ_r is 36.6 J/cm^2. The calculated result of energy dependence by using the equation 2 and 3 is shown in Figures 3 and 8. The best fitting is obtained to be $\sigma_0 = 1 \times 10^{-19}$ cm^2, log $A = 12.84$, and $E_a = 51.7$ kcal/mol for HCl elimination reaction. The absorption cross section(σ_0) obtained from our calculation falls within the range of general value for halogen compound (10^{-18}–10^{-20}). The values for the activation energy and A factor were also in good agreement with the ranges of known values for the HCl elimination reactions (50–56 kcal/mol and 10^{11}–10^{13} s^{-1}). The calculated results show that the dissociation yield per pulse(α) have an 3.0 power energy dependence at low energy and an 1.8 power energy dependence at high energy, higher power energy dependence. The branching ratio was best reproduced when the differences of the activation energies and Arrhenius A factors (log A) for two reaction channels is 1.7 kcal/mol and 0.16, respectively. Using the same procedure, the pressure dependence was calculated by varing the collision efficiency(β) in EGME, with all other input parameters being fixed. The calculated results are shown in Figures 5 and 9. The best fitting was obtained by assuming that the collision efficiency(β) was 0.65.

Acknowledgement. We are grateful for the financial support by the SNU Daewoo Research Fund, and in part by the Korea Science and Engineering Foundation (KOSEF).

References

1. J. I. Steinfeld, Ed., *"Laser-Induced Chemical Processes"*: Plenum: New York, 1981.
2. R. V. Ambarzumian and V. S. Letokhov, *"Chemical and Biochemical Applications of Laser"*; Vol. 2, edited by C. B. Moore (Academic, New York, 1977).
3. Y. Yano, S. Ozaki, H. Ogura and E. Tschuikov-Roux, *J. Phys. Chem.*, **89**, 1108 (1985).
4. P. J. Papagiannakopoulous, K. Kosnik and S. W. Benson, *Int. J. of Chem. Kinetics*, **14**, 327 (1982).
5. M. Quack and H. J. Thone, *Chem. Phys. Lett.*, **135**, 487 (1987).
6. P. A. Hackett, C. Willis, M. Drouin and E. Weinberg, *J. Phys. Chem.*, **84**, 1873 (1980).
7. J. T. Wanna and D. C. Tardy, *J. Phys. Chem.*, **85**, 3749 (1981).
8. Y. Ishikawa, K. Sugita and S. Arai, *J. Phys. Chem.*, **90**, 5067 (1986).
9. W. A. Jalenk, N. S. Norgar, *J. Chem. Phys.*, **79**, 816 (1983).
10. S. Kato, Y. Makide and T. Tominaga, *J. Phys. Chem.*, **91**, 4278 (1987).
11. A. J. Colussi, S. W. Benson, R. J. Hwang and J. J. Tiee, *Chem. Phys. Lett.*, **52**, 349 (1977).
12. A. Lifshitz, M. Frenklach and A. Burcat, *J. Phys. Chem.*, **79**, 1148 (1975).
13. D. R. Keefer, J. E. Allen, Jr. and W. B. Person, *Chem. Phys. Lett.*, **43**, 394 (1976).
14. J. L. Lyman, S. D. Rockwood and S. M. Freund, *J. Chem. Phys.*, **67**, 4545 (1977).
15. S. Mukamel, *J. Chem. Phys.*, **71**, 2012 (1979).
16. K. G. Kay, *J. Chem. Phys.*, **71**, 2012 (1979).
17. J. Stone and M. F. Goodman, *J. Chem. Phys.*, **71**, 408 (1979).
18. M. Quack, *J. Chem. Phys.*, **69**, 1282 (1978).
19. S. Speiser and J. Jortner, *Chem. Phys. Lett.*, **44**, 399 (1976).
20. K. Takeuchi, I. Inoue, R. Nakane, Y. Makide, S. Kato and T. Tominaga, *J. Chem. Phys.*, **76**, 398 (1982).
21. P. J. Robinson and K. A. Holbrook, *"Unimolecular Reaction"*; Willey, New York, 1972.
22. A. T. Blades and G. W. Murphy, *J. Am. Chem. Soc.*, **74**, 6219 (1952).
23. J. C. Jang, D. W. Setser and W. C. Danen, *J. Am. Chem. Soc.*, **104**, 5440 (1982).
24. J. C. Jang-Wren, D. W. Setser and I. C. Ferrero, *J. Phys. Chem.*, **89**, 414 (1985).
25. J. R. Rice, Ed. *"Mathematical Software"*; Academic press: New York, 1971.